PAPER *Special Section on 2006 International Symposium on Antennas and Propagation*

Electromagnetic Scattering Properties in a Multilayered Metamaterial Cylinder

Cheng-Wei QIU[†a)], **Hai-Ying YAO**[††b)], **Shah-Nawaz BUROKUR**[†††], **Saïd ZOUHDI**[†††c)], ***Nonmembers***, ***and*** **Le-Wei LI**[††], ***Member***

SUMMARY Electromagnetic scattering properties of metamaterial cylinders due to a line source are studied by a multilayer algorithm based on eigenfunctional expansion. Closed forms of electric and magnetic fields are formulated. Both the fields inside the cylinder and field in outer space are plotted for different sizes of the cylinder. The focusing phenomena and the wave propagation in the presence of metamaterial cylinders are investigated and shown. Electromagnetic field distributions are presented for subwavelength metamaterial cylinders and cylinders fabricated by magnetoelectric materials, and resonant scattering and focusing properties are reported. Special designs of scatterer cloaking are proposed and calculated by multilayer algorithm which can reduce scattering cross sections.

key words: *multilayer algorithm, metamaterial, magnetoelectric coupling, subwavelength cylinder, cloaking*

1. Introduction

The permeability and permittivity of a material are two of the fundamental parameters that determine how the material interacts with electromagnetic (EM) waves propagating and scattering in the materials. Metamaterials, with simultaneously negative permittivity and permeability in a frequency band, have received intensive interests, which exhibit a lot of exotic properties (e.g., reversal Doppler shift and negative refraction [1], reversed circular Bragg phenomenon [2] and perfect lens [3]). These materials exhibit a left-handed rule which are referred to as left-handed materials (LHM) in literature [4]–[6]. The double negative (DNG) material has shown special optical properties, and could lead to a perfect lens [7], [8].

The plane wave propagating through layered DNG media were formulated by Kong [9] for planar structures. In this paper, existing application is extended to the line-source incidence associated with cylindrical multilayers, so as to gain more insight into the hybrid effects of metamaterials and cylindrical curvature. Eigenfunction expansion technique [10]–[12] is employed to establish a systematic scheme, which can incorporate the material functionality, the geometrical parameters and incidence characteristics together. By using the multilayer algorithm, single cylinders are considered so as to investigate the subwavelength imaging and wave interaction. Different kinds of metamaterial single cylinders are studied. Interesting results such as focusing properties and energy localization are shown. Next, we further study the cylinder with magnetoelectric coupling as a special case. In this case, the cylinder is characterized by 3 parameters: permittivity, permeability and chirality. The effect of magnetoelectric coupling is presented and resonant scattering is discussed. Finally, the cloaking of cylinders and its effects on cross section are examined.

2. Preliminaries

2.1 Eigenfunction Expansion

Consider a parallel infinite line source with electric current I, which is placed at (ρ_0,ϕ_0) from the cylinder as depicted in Fig. 1. The incident field due to the line source can be expressed

$$\boldsymbol{E}^i = -\frac{k^2 I}{4\omega\varepsilon_0}\sum_{n=0}^{\infty}(2-\delta_{n0})\,H_n^{(1)}(k\rho_0)\,\boldsymbol{N}_n^{(1)}(k)\,e^{-jn\phi_0} \tag{1}$$

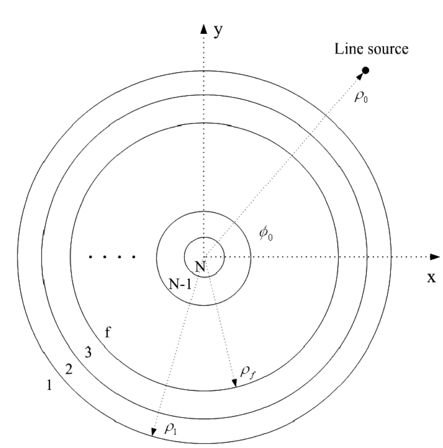

Fig. 1 Cross-section view of a multilayered cylinder with the line source in 1st region.

Manuscript received December 26, 2006.
Manuscript revised February 17, 2007.

[†]The author is with the Department of Electrical and Computer Engineering, National University of Singapore, and also with Ecole Supérieure D'Électricité, France.
[††]The authors are with the Department of Electrical and Computer Engineering, National University of Singapore.
[†††]The authors are with the Laboratoire de Génie Électrique de Paris, Ecole Supérieure D'Électricité, France.
a) E-mail: chengweiqiu@nus.edu.sg
b) E-mail: eleyh (elelilw, eleyeots)@nus.edu.sg
c) E-mail: sz@ccr.jussieu.fr

DOI: 10.1093/ietcom/e90–b.9.2423

$$\boldsymbol{H}^i = -\frac{kI}{4j}\sum_{n=0}^{\infty}(2-\delta_{n0})\,H_n^{(1)}(k\rho_0)\,\boldsymbol{M}_n^{(1)}(k)\,e^{-jn\phi_0} \tag{2}$$

where the vector wave functions (VWFs) have been given in [13], [14]

$$\boldsymbol{N}_n^{(1)}(k) = \widehat{\boldsymbol{z}}J_n(k\rho)e^{jn\phi} \tag{3}$$

$$\boldsymbol{M}_n^{(1)}(k) = \left[\widehat{\boldsymbol{\rho}}\frac{jn}{k\rho}J_n(k\rho) - \widehat{\boldsymbol{\phi}}J_n'(k\rho)\right]e^{jn\phi}. \tag{4}$$

One can however note that the superscript of VWFs would change to 3 if the multiple reflection and transmission are taken into accout due to the interfaces in Fig. 1:

$$\boldsymbol{N}_n^{(3)}(k) = \widehat{\boldsymbol{z}}H_n^{(1)}(k\rho)e^{jn\phi} \tag{5}$$

$$\boldsymbol{M}_n^{(3)}(k) = \left[\widehat{\boldsymbol{\rho}}\frac{jn}{k\rho}H_n^{(1)}(k\rho) - \widehat{\boldsymbol{\phi}}H_n'^{(1)}(k\rho)\right]e^{jn\phi}. \tag{6}$$

Based on the eigenfunction expansion, the electromagnetic fields in intermediate layers (e.g., fth layer) are as follows

$$\boldsymbol{E}_f = \sum_{n=0}^{\infty}\Big\{a_{nf}\boldsymbol{N}_n^{(3)}\left(k_{zf}\right) + b_{nf}\boldsymbol{M}_n^{(3)}\left(k_{zf}\right) + a'_{nf}\boldsymbol{N}_n^{(1)}\left(k_{zf}\right) + b'_{nf}\boldsymbol{M}_n^{(1)}\left(k_{zf}\right)\Big\}, \tag{7}$$

$$\boldsymbol{H}_f = \frac{1}{j\eta_f}\sum_{n=0}^{\infty}\Big\{a_{nf}\boldsymbol{M}_n^{(3)}\left(k_{zf}\right) + b_{nf}\boldsymbol{N}_n^{(3)}\left(k_{zf}\right) + a'_{nf}\boldsymbol{M}_n^{(1)}\left(k_{zf}\right) + b'_{nf}\boldsymbol{N}_n^{(1)}\left(k_{zf}\right)\Big\}. \tag{8}$$

In Eq. (7), scattering coefficients a'_{nf} and b'_{nf} denote incoming TM and TE modes (Bessel function being convergent approaching the origin), and a_{nf} and b_{nf} represent outgoing TM and TE modes (Hankel function being finite in the infinity). Therefore, in the 1st region, the scattered electric field only contains Hankel function. In Nth region, the scattered electric field only contains Bessel function. This is the principle of eigenfunction expansion. In the intermediate layers, the fields are just the superposition of inward and outward scattered fields due to the multiple interfaces. Note that k_{zf} and $\eta_f = k_f/\omega\mu_f$ denote longitudinal wavenumber and wave impedance in fth layer, respectively. $k_f^2 = \omega^2\mu_f\epsilon_f$ is the wavenumber for incidence at arbitrary angles, and it reads $k_f^2 = k_\rho^2 + k_z^2$ where k_ρ is the radial wavenumber in fth layer.

Those scattering coefficients can be solved in a multilayer algorithm associated with boundary conditions at each interface, which will be shown later. Thus, we can have the electromagnetic field expansions based on the field coupling together with the incoming/outgoing waves superposition. The electric fields in 1st and Nth layer are given, respectively

$$\boldsymbol{E}_1 = \boldsymbol{E}^i + \sum_{n=0}^{\infty}\Big\{a_{n1}\boldsymbol{N}_n^{(3)}(k_{z1}) + b_{n1}\boldsymbol{M}_n^{(3)}(k_{z1})\Big\} \tag{9}$$

$$\boldsymbol{E}_N = \sum_{n=0}^{\infty}\Big\{a'_{nN}\boldsymbol{N}_n^{(1)}(k_{zN}) + b'_{nN}\boldsymbol{M}_n^{(1)}(k_{zN})\Big\}. \tag{10}$$

Note that the vectors $\boldsymbol{M}(k)$ and $\boldsymbol{N}(k)$ have the following relations

$$\nabla\times\boldsymbol{M}(k) = k\boldsymbol{N}(k) \tag{11}$$

$$\nabla\times\boldsymbol{N}(k) = k\boldsymbol{M}(k). \tag{12}$$

Therefore, the magnetic fields in 1st and Nth can be obtained as follows

$$\boldsymbol{H}_1 = \boldsymbol{H}^i + \frac{1}{j\eta_1}\sum_{n=0}^{\infty}\Big\{a_{n1}\boldsymbol{M}_n^{(3)}(k_{z1}) + b_{n1}\boldsymbol{N}_n^{(3)}(k_{z1})\Big\} \tag{13}$$

$$\boldsymbol{H}_N = \frac{1}{j\eta_N}\sum_{n=0}^{\infty}\Big\{a'_{nN}\boldsymbol{M}_n^{(1)}(k_{zN}) + b'_{nN}\boldsymbol{N}_n^{(1)}(k_{zN})\Big\}. \tag{14}$$

2.2 Multilayer Algorithm

The electromagnetic fields satisfy the boundary conditions at each interface $\rho = \rho_f$

$$\widehat{\boldsymbol{\rho}}\times\begin{bmatrix}\boldsymbol{E}_f\\ \boldsymbol{H}_f\end{bmatrix} = \widehat{\boldsymbol{\rho}}\times\begin{bmatrix}\boldsymbol{E}_{(f+1)}\\ \boldsymbol{H}_{(f+1)}\end{bmatrix}. \tag{15}$$

Inserting Eqs. (7) and (8) into Eq. (15), we have a linear equation

$$\left[F_f\right]\left[C_f\right] = \left[F_{(f+1)}\right]\left[C_{(f+1)}\right] \tag{16}$$

where $\left[F_f\right]$ is a 4×4 matrix

$$\left[F_f\right] = \begin{bmatrix}F_{f1}\\ F_{f2}\\ F_{f3}\\ F_{f4}\end{bmatrix} \tag{17}$$

with the definition

$$\left[F_{f1}\right] = \begin{bmatrix}0 & -H_n'^{(1)}(k_f\rho) & 0 & -J_n'(k_f\rho)\end{bmatrix}$$

$$\left[F_{f2}\right] = \begin{bmatrix}-H_n^{(1)}(k_f\rho) & 0 & -J_n(k_f\rho) & 0\end{bmatrix}$$

$$\left[F_{f3}\right] = \begin{bmatrix}-\frac{H_n'^{(1)}(k_f\rho)}{j\eta_f} & 0 & -\frac{J_n'(k_f\rho)}{j\eta_f} & 0\end{bmatrix}$$

$$\left[F_{f4}\right] = \begin{bmatrix}0 & -\frac{H_n^{(1)}(k_f\rho)}{j\eta_f} & 0 & -\frac{J_n(k_f\rho)}{j\eta_f}\end{bmatrix}.$$

Note that the derivative is with respect to the argument. The $\left[C_f\right]$ is a vector of unknown scattering coefficients

$$\left[C_f\right] = \begin{bmatrix}a_{nf} & b_{nf} & a'_{nf} & b'_{nf}\end{bmatrix}^T. \tag{18}$$

By defining a new matrix

$$\left[T_f\right] = \left[F_{f+1}\right]^{-1}\left[F_f\right], \tag{19}$$

we can rewrite

$$[C_N] = \left[T_N^{(1)}\right][C_1] \tag{20}$$

where

$$\left[T_N^{(f)}\right] = \left[T_{N-f}\right]\left[T_{N-(f+1)}\right]\ldots[T_2]\,[T_1]. \tag{21}$$

Therefore, the coefficient relationship between inner- and outer-most layer can be established

$$\begin{bmatrix} 0 \\ 0 \\ a'_{nN} \\ b'_{nN} \end{bmatrix} = \left[T_N^{(1)}\right] \begin{bmatrix} a_{n1} \\ b_{n1} \\ a'_{n1} \\ b'_{n1} \end{bmatrix}. \tag{22}$$

In view of Eq. (1), we have

$$a'_{n1} = -(2-\delta_{n0}) \frac{k_1^2 I}{4\omega\varepsilon_0} H_n^{(1)}(k_1\rho_0)\, e^{-jn\phi_0}, \tag{23}$$

$$b'_{n1} = 0 \tag{24}$$

where k_1 is just the wave number in free space. Since a'_{n1} and b'_{n1} are already known, a_{n1} and b_{n1} can be determined via the first two rows of $\left[T_N^{(1)}\right]$ in Eq. (22), regardless of the value of a'_{nN} and b'_{nN}. Provided $[C_1]$ is obtained, $\left[C_f\right]$ is straightforward by using Eq. (21). As a result, electromagnetic fields in any region can be formulated.

2.3 Magnetoelectric Coupling

To consider a more general case, the dielectric material is just a subset of the bi-isotropic material, which exhibit magnetoelectric coupling in the form of

$$\boldsymbol{D} = \epsilon_r\epsilon_0 \boldsymbol{E} + j\kappa\sqrt{\epsilon_0\mu_0}\boldsymbol{H} \tag{25}$$

$$\boldsymbol{B} = -j\kappa\sqrt{\epsilon_0\mu_0}\boldsymbol{E} + \mu_r\mu_0\boldsymbol{H} \tag{26}$$

where the chirality κ denotes the degree of magnetoelectric coupling.

Lindell et al have presented the wavefield decomposition method in [15]. Instead of treating the electromagnetic problems in bi-isotropic media directly, the field components can be split into two partial fields

$$\boldsymbol{E} = \boldsymbol{E}_+ + \boldsymbol{E}_- \tag{27}$$

$$\boldsymbol{H} = \boldsymbol{H}_+ + \boldsymbol{H}_- \tag{28}$$

with a pair of equivalent isotropic mediums:

$$\epsilon_\pm = \epsilon(1 \pm \kappa) \tag{29}$$

$$\mu_\pm = \mu(1 \pm \kappa). \tag{30}$$

Hence, the previous formulated algorithm can still work even for bi-isotropic media. As a special case, chiral nihility was proposed by Tretyakov et al. in [16] to achieve backward wave and negative refraction. Later on, Qiu et al studied the energy transport in the chiral nihility and revisited the condition of chiral nihility for slabs in [17]. In this paper, we further extend our study on chiral nihility to cylindrical structures with the possibility of imaging and negative rafraction due to cylindrical curvatures. The chirality effect on subwavelength imaging will be discussed in detail in the following section.

3. Results and Discussion

In this section, only one-layer and two-layer cylinders are considered because they possess enough interesting scattering properties. The present work can be extended to study 3-layer or 4-layer cylinders straightforwardly since the multilayer algorithm developed above is suitable for arbitrary layers.

3.1 One-Layer Isotropic Cylinder

First, let us investigate the scattering properties in the presence of one-layer isotropic cylinder due to the line-source radiation. The material inside the cylinder in Fig. 2 is anti-vacuum (i.e, $\epsilon = -\epsilon_0$ and $\mu = -\mu_0$). The line source is placed at the position of $(4.5\lambda, 0°)$, which is very close to the surface of cylinder. As is known, a slab filled with anti-vacuum can act as a perfect lens to focus light. However, if we consider perfect cylindrical lens, the parameters of the filling material must be dependent on the position. Nevertheless, partial focusing phenomenon can still be observed in Fig. 2. Also, some reflection can be observed at the positions behind the line source in Fig. 2 because of the cylindrical curvature. It can be seen that ripple occurs at the cylinder's surface close to the line source, which is the incoming window of the incident wave. Certain points of this ripple carry comparably high energy as the line source. In Fig. 3 and Fig. 4, the line source is put further away to the cylinder's surface, while the radius of the cylinder keep unchanged. When the source is far away from the surface, the ripple effect in the incoming window on the cylinder will be reduced as expected. In Fig. 3 and Fig. 4, foculas are formed due to the imperfect focusing condition. By changing the position of line source, the energy distributions outside the cylinder are greatly modified as can be seen from Fig. 2 to Fig. 4. It is due to the fact that when the line source is very close to the cylinder's surface, the curvature is quite flat within the incoming window of incident wave, which is close to slab configuration. If the line source is moved faraway, the incoming window becomes larger and the cylindrical curvature takes effect.

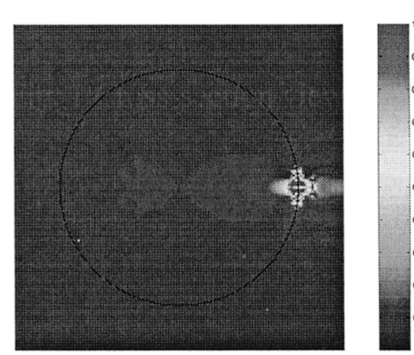

Fig. 2 Normalized magnitude of Poynting vector of a cylinder of $a = 4\lambda$ filled with anti-vacuum and the line source at $(4.5\lambda, 0°)$.

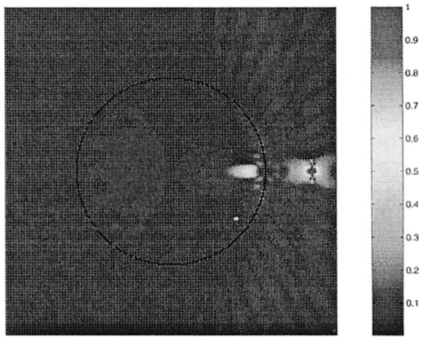

Fig. 3 Normalized magnitude of Poynting vector of the same cylinder as in Fig. 2 except the line source at (6λ, $0°$).

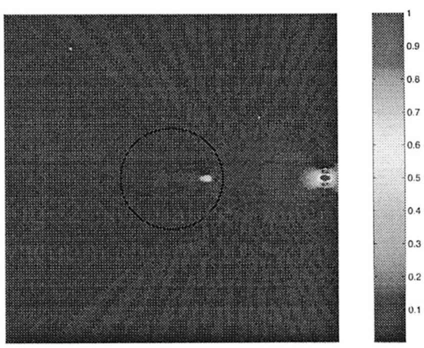

Fig. 4 Normalized magnitude of Poynting vector of the same cylinder as in Fig. 2 except the line source at (12λ, $0°$).

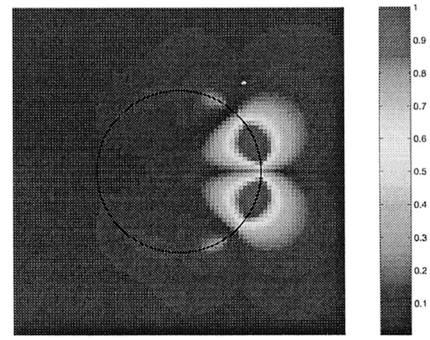

Fig. 5 Normalized magnitude of Poynting vector of a cylinder of $a = 0.05\lambda$ filled with anti-vacuum and the line source at (0.25λ, $0°$).

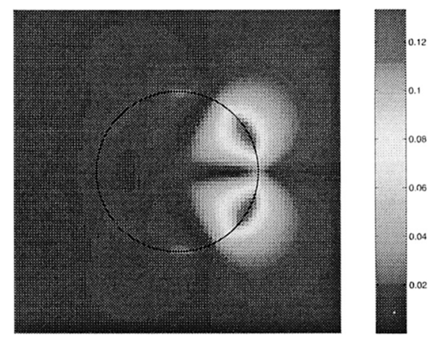

Fig. 6 Normalized magnitude of Poynting vector of a cylinder of $a = 0.05\lambda$ filled with anti-vacuum and the line source at (1.05λ, $0°$).

We further investigate scattering properties of subwavelength cylinders due to the line source radiation. The radii in Fig. 5 and Fig. 6 are both equal 0.05λ, while the distance of line source from the surface is 0.2λ and 1λ, respectively. Note that the energy distribution around the line source is suppressed and only the distribution near the cylinder is plotted. Two foculas with giant energy distribution are found in Fig. 5 when the distance of line source from the surface is four times of the radius. Of particular interest is that the focula is not located inside the subwavelength cylinder any more. Instead, the foculas are formed in two particular areas around the cylindrical surface. If the distance of line source increase to 20 times of radius (see Fig. 6), the magnitude of the two foculas decrease and the positions are more apart from each other.

3.2 One-Layer Bi-isotropic Cylinder

Now the bi-isotropic cylinder with magnetoelectric couplings, as described by Eqs. (25) and (26), is studied. The degree of magnetoelectric couplings is represented by the chirality of κ. Different chiralities are chosen so as to study the effect of magnetoelectric coupling upon the scattering properties of the cylinder.

As a special case of bi-isotropic media, chiral nihility is considered first since it yields two special equivalent mediums: one is vacuum and the other is anti-vacuum, which can be verified in Eqs. (29) and (30). The judicious selection of parameters for chiral nihility is based on the findings in [17]. It is shown in Fig. 7 that there are several foculas inside the cylinder and both energy distributions inside and outside the cylinder are greatly modified by the existence of magnetoelectric couplings. Compared with Fig. 3, the energy in Fig. 7 behind the cylinder is enhanced and those enhanced distributions forms some ribbon-shaped areas.

In what follows, we consider normal bi-isotropic mediums with the same ϵ_r and μ_r, but different κ. The reason why $\epsilon_r = \mu_r$ is that the wave impedance of bi-isotropic medium is independent of κ and identical with the impedance of free space. From the comparison between Fig. 8 and Fig. 9, it can be seen that the focusing appears more obvious for bigger κ value. More interestingly, in Fig. 9, it not only presents two focusing points, but also enhance the energy inside the cylinder and high energy distribution is confined along the diameter.

3.3 Cloaking for Subwavelength Cylinders

Here the cloaking for a thin cylinder and its selection of parameters are studied. We consider two combinations of the core and cloaking layers: double positive against double negative pair (DPS-DNG) and epsilon negative against mu negative pair (ENG-MNG). Such combinations may give rise to the interface resonances, provided proper choice of radii ratios. In analogy with what have been noticed for thin planar resonators [18], [19], the condition of having a no-

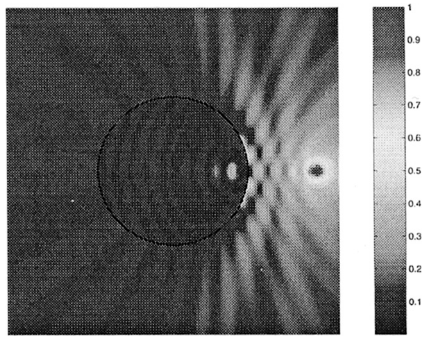

Fig. 7 Normalized magnitude of Poynting vector of a bi-isotropic cylinder of $a = 2.5\lambda$ filled with chiral nihility medium of $\epsilon_r = 1e{-}5$, $\mu_r = 1e{-}5$, and $\kappa = 1$ and the line source at $(4.8\lambda, 0°)$.

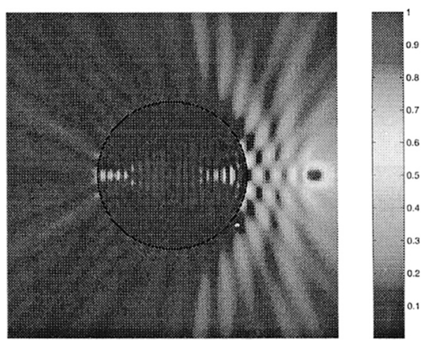

Fig. 8 Normalized magnitude of Poynting vector of a cylinder of $a = 2.5\lambda$ filled with bi-isotropic medium of $\epsilon_r = 1$, $\mu_r = 1$, and $\kappa = 2$ and the line source at $(4.8\lambda, 0°)$.

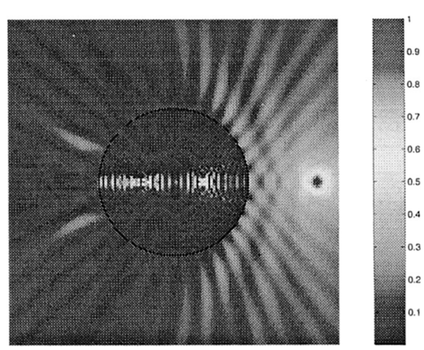

Fig. 9 Normalized magnitude of Poynting vector of a cylinder of $a = 2.5\lambda$ filled with bi-isotropic medium of $\epsilon_r = 1$, $\mu_r = 1$, and $\kappa = 4$ and the line source at $(4.8\lambda, 0°)$.

cut-off propagation mode in a thin cloaking cylinder filled with a pair of DPS-DNG or ENG-MNG layers, depends on the ratio of the radii of the core cylinder (i.e., ρ_2) and the cloaking layer (i.e., ρ_1) instead of the sum of radii or the outer radius. As shown in Fig. 10, a cloaking cylinder consists of 2 layers (i.e., 3 regions). The radius of the cloaking is ρ_1 and the radius of the core-cylinder is ρ_2. The line source is placed at ($\rho_0 = 0.8\lambda$, $\phi_0 = 0°$). The outer radius of the cloaking layer is fixed to be $\rho_1 = 0.01\lambda$ and scattering cross section (SCS) is plotted against the radii ratio in order to find resonances. SCS is defined as the ratio of the power

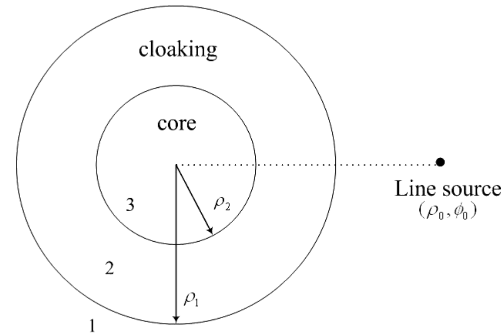

Fig. 10 Scattering cross section versus ratio of core layer over cloaking layer in two pairs of combinations: DNG-DPS and DPS-DPS. The outer space is free space.

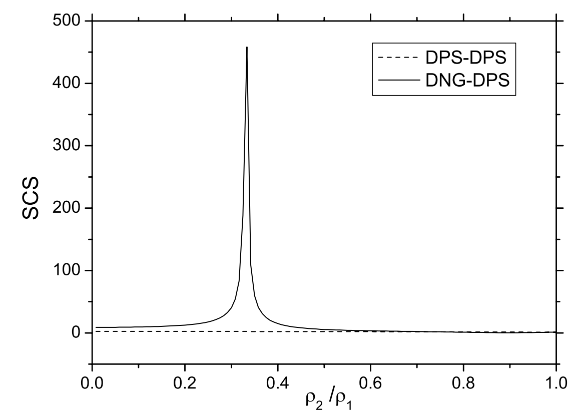

Fig. 11 Scattering cross section versus ratio of core layer over cloaking layer in two pairs of combinations: DNG-DPS and DPS-DPS. In the case of DNG-DPS pairing, the cloaking layer is filled with DNG medium of $(-3\epsilon_0, -2\mu_0)$, and in the case of DPS-DPS pairing, the cloaking layer is filled with DPS medium of $(3\epsilon_0, 2\mu_0)$. The core layer remains the same DPS medium of $(2\epsilon_0, \mu_0)$ for both pairings.

scattered by the scatterer to the incident power per unit area

$$\mathrm{SCS} = \frac{\frac{1}{2}\mathrm{Re}[E^{sca} \times H^{sca*}]}{\frac{1}{2}\mathrm{Re}[E^{inc} \times H^{inc*}]} \tag{31}$$

In Fig. 11, the dash line refers to the case that both the core and cloaking layers are DPS mediums. Hence, we can see that the SCS is very small since the geometry of this scatter is in subwavelength size. Note that the SCS of dash line is very close to zero, but not exactly zero because we plot DNG-DPS in the same figure as well. Interestingly, a resonant ratio can be observed for DNG-DPS pairing at $\rho_2/\rho_1 \approx 0.331$, where the SCS is significantly enhanced. It is attributed to the polaritons which are supported by this pairing. It also shows that a proper cloaking on a subwavelength conventional cylinder can yield a comparably large scattering width similar to that obtained from very thick cylinder. Therefore, the scattering properties of a geometrically small cylindrical scatterer can be amplified up to a big scatterer, if the cloaking material and the ratio of radii are properly chosen.

Analogous scattering properties are obtained for ENG-MNG cloakings. In the solid line in Fig. 12, core layer is

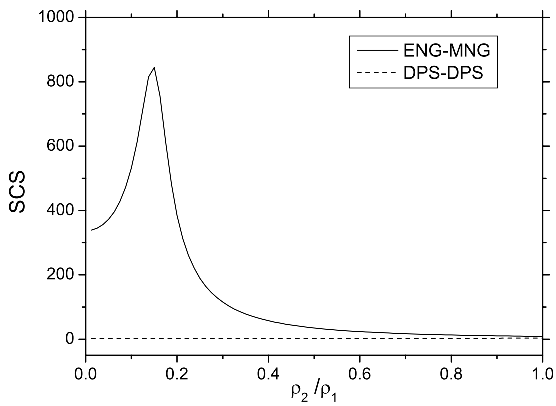

Fig. 12 Scattering cross section versus ratio of core layer over cloaking layer in two pairs of combinations: ENG-MNG and DPS-DPS. In the case of ENG-MNG pairing, the cloaking layer is filled with ENG medium of $(-3\epsilon_0, \mu_0)$, while core layer is occupied by MNG medium of $(4\epsilon_0, -2\mu_0)$. In the case of DPS-DPS pairing, the cloaking and core layers are filled with DPS medium of $(3\epsilon_0, \mu_0)$ and $(4\epsilon_0, 2\mu_0)$, respectively.

a mu-negative cylinder while the cloaking is an epsilon-negative coating. Resonant ratio can be found at $\rho_2/\rho_1 \approx 0.152$. In contrast to DNG-DPS pairing, the resonant scattering in Fig. 12 is not as sensitive to ratio as in Fig. 11. By coating a MNG subwavelength cylinder by an ENG cloaking, the scattering is still much amplified compared to DPS-DPS combination even if the radii ratio is smaller than the resonant ratio at about 0.152. However, when the inner radius ρ_2 of MNG core layer keeps increasing, the scattering cross section will reduce to that of DPS-DPS combination as the dash line in Fig. 12.

4. Conclusion

In this paper, a multilayer algorithm is proposed to study the scattering properties of multilayered metamaterial cylinders by the radiation of a line source. The algorithm can treat arbitrary layers with arbitrary filling dielectric materials. Both single isotropic/bi-isotropic subwavelength cylinder and subwavelength cloaking cylinders are investigated. Focusing phenomena and enhanced resonant scattering are presented.

Acknowledgments

The authors are grateful to the support from SUMMA Foundation in US and French-Singaporean Merlion Project. C.-W. Qiu is also grateful to the Joint PhD Degree Programme offered by National University of Singapore, in Singapore, and Supélec, in Paris, France.

References

[1] V.G. Veselago, "The electrodynamics of substances with simultaneously negative values of ε and μ," Soviet Physics Uspekhi, vol.10, no.4, pp.509–514, 1968.
[2] A. Lakhtakia, "Handedness reversal of circular Bragg phenomenon due to negative real permittivity and permeability," Opt. Express, vol.11, no.7, pp.716–722, 2003.
[3] J.B. Pendry, "Negative refraction makes a perfect lens," Phys. Rev. Lett., vol.85, pp.3966–3969, 2000.
[4] A. Grbic and G.V. Eleftheriades, "Overcoming the diffraction limit with a planar left-handed transmission-line lens," Phys. Rev. Lett., vol.92, 117403, 2004.
[5] R.W. Ziolkowski and A.D. Kipple, "Causality and double-negative metamaterials," Phys. Rev. E, vol.68, 026615, 2003.
[6] C.W. Qiu, H.Y. Yao, L.W. Li, S. Zouhdi, and T.S. Yeo, "Backward waves in magnetoelectrically chiral media: Propagation, impedance, and negative refraction," Phys. Rev. B, vol.75, 155120, 2007.
[7] J.B. Pendry, "Perfect cylindrical lenses," Opt. Express, vol.11, no.7, pp.755–760, 2003.
[8] S.A. Ramakrishna and J.B. Pendry, "Spherical perfect lens: Solutions of Maxwell's equations for spherical geometry," Phys. Rev. B, vol.69, 115115, 2004.
[9] J.A. Kong, "Electromagnetic wave interaction with stratified negative isotropic media," Prog. Electromagn. Res., vol.35, pp.315–334, 2002.
[10] L.W. Li, P.S. Kooi, M.S. Leong, L.W. Li, and S.L. Ho, "On the eigenfunction expansion of dyadic Green's functions in rectangular cavities and waveguides," IEEE Trans. Microw. Theory Tech., vol.43, no.3, pp.700–702, 1995.
[11] C.W. Qiu, L.W. Li, H.Y. Yao, and S. Zouhdi, "Properties of Faraday chiral media: Green dyadics and negative refraction," Phys. Rev. B, vol.74, 115110, 2006.
[12] C.W. Qiu, H.Y. Yao, L.W. Li, S. Zouhdi, and T.S. Yeo, "Eigenfunctional representation of dyadic Green's functions in multilayered gyrotropic chiral media," J. Phys. A, Math. Theor., vol.40, no.21, pp.5751–5766, 2007.
[13] C.T. Tai, Dyadic Green's Functions in Electromagnetic Theory, 2nd ed., IEEE Press, Piscataway, NJ, 1994.
[14] L.W. Li, S.N. Lim, M.S. Leong, and J.A. Kong, "Vector wave function expansion for dyadic Green's functions for cylindrical chirowaveguides: An alternative representation," J. Electromagn. Waves Appl., vol.14, no.5, pp.673–692, 2000.
[15] I.V. Lindell, A.H. Sihvola, S. A Tretyakov, and A.J. Viitanen, Electromagnetic Waves in Chiral and Bi-isotropic Media, Artech House, Boston/London, 1994.
[16] S. Tretyakov, I. Nefedov, A. Sihvola, S. Maslovski, and C. Simovski, "Waves and energy in chiral nihility," J. Electromagn. Waves Appl., vol.17, no.5, pp.695–706, 2003.
[17] C.W. Qiu, N. Burokur, S. Zouhdi, and L.W. Li, "Study on energy transport in chiral nihility and chirality nihility effects," submitted to J. Opt. Soc. Am. A, 2006.
[18] N. Engheta, "An idea for thin subwavelength cavity resonators using metamaterials with negative permittivity and permeability," IEEE Antennas Wirel. Propag. Lett., vol.1, no.1, pp.10–13, 2002.
[19] A. Alù and N. Engheta, "Pairing an epsilon-negative slab with a mu-negative slab: Resonance, tunneling and transparency," IEEE Trans. Antennas Propag., vol.51, no.10, pp.2558–2571, Oct. 2003.

Cheng-Wei Qiu was born in Zhejiang, China, on March 9, 1981. He received the B.Eng. degree from the University of Science and Technology of China, Hefei, China, in 2003. In August 2003, he was admitted by the PhD program in National University of Singapore (NUS) in Singapore. Currently, he is working at Laboratoire de Génie Electrique de Paris-Supélec, under the NUS-Supélec Joint PhD Programme. His research interests are in the areas of electromagnetic wave theory, composite functional materials, and metamaterial antennas. He was the recipient of SUMMA Graduate Fellowship in Advanced Electromagnetics for Year 2005. He was also the recipient of IEEE AP-S Graduate Research Award in 2006. In 2007, he received the Young Scientist Travel Grant for ISAP2007 in Niigata, Japan and Travel Grant for Metamaterial'07 in Rome, Italy.

Hai-Ying Yao received the B.Eng. degree in electronic engineering, and M.Eng. degree and Ph.D. degree both in Electromagnetic Field and Microwave Technology all from University of Electronic Science and Technology of China (UESTC), Chengdu, China, in 1996, 1999, and 2002, respectively. From April 2000 to October 2001, she worked at City University of Hong Kong, as a Research Assistant. From December 2002 to September 2004, she worked at High Performance Computations on Engineered Systems Programme of Singapore-MIT Alliance (SMA) as a Research Fellow. Since Oct. 2004, she has been a Research Fellow with the Department of Electrical and Computer Engineering at the National University of Singapore. Her current research interests include fast algorithms and hybrid methods in computational electromagnetics, radio wave propagation and scattering in various media, and analysis and design of various antennas.

Shah-Nawaz Burokur was born in Mauritius in 1978. He received the DEA (Master) degree in microwave engineering from the University of Rennes1, France, in 2002. In 2005, he received the Ph.D. degree from the University of Nantes, France. His Ph.D. research works dealt with the applications of Split Ring Resonators (SRR) to microwave devices and antennas. From September 2005 to August 2006, he was a post-doctoral research fellow at the Laboratoire de Génie Electrique de Paris where he worked on chiral metamaterials. He is actually a post-doctoral research fellow at the Institut d'Electronique Fondamentale (IEF) - University of Paris Sud, France. His current research interests are in the areas of microwave and applications of periodic structures, complex media, metamaterials and metasurfaces, in the analysis of integrated planar and conformal circuits and antennas. Dr. Burokur has been the recipient of the Young Scientist Award, presented by the Union Radio-Scientifique Internationale (URSI) Commission B, in 2005. He serves as reviewer of the IET Microwaves, Antennas and Propagation and the Journal of Electromagnetic Waves and Applications. He is currently a member of the European Network of Excellence METAMORPHOSE.

Saïd Zouhdi received the Ph.D. degree in Electronics from the University of Pierre et Marie Curie, France, in 1994 and the Habilitation in Electrical Engineering from the University Paris Sud, France in 2003. He has been with the Laboratoire de Génie Electrique de Paris at Supélec. He is currently a Professor of electrical engineering at the University Paris Sud. His research interests include electromagnetic wave interaction with complex structures and antennas, electromagnetics of unconventional complex materials such as metamaterials, chiral, bianisotropic and PBG materials, and optimization methods for various designs. He is an Editor of the journal Metamaterials. He has published over 100 journal papers, book chapters, and conference articles. He has organized 2 NATO Advanced Research Workshops and organized and chaired various special sessions in international symposia and conferences, and has guest edited/co-edited 3 special issues. He has co-edited the first book on metamaterials "Advances in Electromagnetics of Complex Media and Metamaterials" Kluwer Academic Publishers, in 2003. Prof. Zouhdi is a senior member of the IEEE Antennas and Propagation Society.

Le-Wei Li received the Ph.D. degree in electrical engineering from Monash University, Melbourne, Australia, in 1992. In 1992, he was jointly affiliated with the Department of Electrical and Computer Systems Engineering, Monash University, and the Department of Physics, La Trobe University, Melbourne, Australia, where he was a Research Fellow. Since 1992, he has been with the Department of Electrical and Computer Engineering, National University of Singapore (NUS), Singapore, where he is currently a Professor and Director of the NUS Centre for Microwave and Radio Frequency. From 1999 to 2004, he worked part time with the High Performance Computations on Engineered Systems (HPCES) Programme of SingaporeMIT Alliance (SMA) as an SMA Faculty Fellow. His current research interests include EM theory, computational electromagnetics, radio wave propagation and scattering in various media, microwave propagation and scattering in tropical environment, and analysis and design of various antennas. Within these areas, he coauthored Spheroidal Wave Functions in Electromagnetic Theory (Wiley, 2001), 45 book chapters, over 250 international refereed journal papers (of which over 70 papers were published in IEEE journals and the remaining in Physical Review E, Statistical Physics and Plasmas Fluids Related Interdisciplinary Topics, Radio Science, Proceedings of the IEE, and the Journal of Electromagnetic Waves and Applications (JEWA), 31 regional refereed journal papers, and over 260 international conference papers. As a regular reviewer of many archival journals, he is an overseas Editorial Board member of the Chinese Journal of Radio Science, an Associate Editor of JEWA and the EMW Publishing book series Progress In Electromagnetics Research (PIER), and an Associate Editor of Radio Science. He is also on the Editorial Board of the Electromagnetics Journal. Dr. Li has been a member of The Electromagnetics Academy since 1998. He is an Editorial Board member of the IEEE Transactions on Microwave Theory and Techniques. He was the past chairman of the IEEE Singapore Microwave Theory and Techniques (MTT)/Antennas and Propagation (AP) Joint Chapter during 2002C2003, during which time the 2003 IEEE Antennas and Propagation Society (IEEE AP-S) Best Chapter Award was presented to the Singapore Chapter. He was also the recipient of the 2004 University Excellent Teachers Award presented by NUS. He was also the recipient of several other awards.